Available online at www.sciencedirect.com

ScienceDirect

Procedia Structural Integrity 12 (2018) 145–164

Structural Integrity Procedia

www.elsevier.com/locate/procedia

AIAS 2018 International Conference on Stress Analysis

FEM thermal analysis of a semi-active differential

T. Novi[a], C. Carcasci[a], C. Certosini[a,*], R. Capitani[a], C. Annicchiarico[b]

[a]*Università degli Studi di Firenze - Dipartimento di Ingegneria Industriale, Via di Santa Marta 3, 50139 Firenze, Italy*
[b]*Meccanica 42 s.r.l., Via Madonna del Piano 6, 50019 Sesto fiorentino (FI), Italy*

Abstract

A semi-active differential (SAD) is a device which allows the flaws of a standard limited slip differential (LSD) to be overcome in terms of how they affect vehicle dynamics. This is possible by controlling continuously the locking percentage. A thermal analysis of a semi-active differential (SAD) is presented. An internal electro-hydraulic clutch produces a resistant torque in the analysed device, therefore, the locking percentage is highly influenced by temperature. Steady and transient conditions are evaluated under various conditions of actuation system pressure and relative rotational velocity between the clutch's discs. The radial and axial temperature distribution together with the temperature gradient along the contact surfaces generating friction have been characterized, including the case of a duty cycle.

Keywords: Semi-active differential; Thermal FEM; Unsteady state; Heat transfer; Axisymmetric; Wet Clutch

1. Introduction

In the automotive and motorsport fields, there has been great focus in the past years on the development of active systems to control vehicle behaviour, thus improving handling and safety. This has been enhanced by the increasing integration between different engineering sectors such as mechanics and electronics. One of these devices is the semi-active differential (SAD). This differential allows the amount of locking percentage to be controlled through the use of a hydraulic actuator. Control is completely electronic and governed by a bespoke ECU. The possibility of controlling the locking percentage is what makes this differential an upgrade to the standard limited slip differential (LSD) mounted on most racing vehicles since it improves the understeer/oversteer balance of the car, specifically in conditions such as braking in turn and power on cornering. In order to fully control the friction torque generated by the clutch it is important to know the local friction coefficient. However, since friction is a non-conservative force there is a great amount of heat generated. Such heat obviously tends to raise the temperature of the discs, varying the friction coefficient and, therefore, the amount of redistributed torque. There are multiple other factors

* Corresponding author. Tel.: +39-055-275-8707
E-mail address: cesare.certosini@unifi.it

2452-3216
10.1016/j.prostr.2018.11.099

which influence the friction coefficient between two adjacent discs, such as wear (see Tesi et al. (2016)) difference in rotational speed, difference in slip velocity along the disc radius and elasticity of material. The dependence of friction coefficient on temperature can be explained since fluid viscosity is affected by temperature and the formation of so-called tribolayers (see Mäki (2005); Hsu and Gates (2005); Rudnick (2017)). The relationship between friction and temperature and, specifically its dependence, shows that, for most materials, the friction coefficient tends to decrease as temperature rises. This has been verified by many experimental methods, for instance by using a modified SAE No. 2 machine as done by Ohtani et al. (1994) or a low velocity friction apparatus also known as LVFA as done by Watts and Nibert (1992), and Haviland and Rodgers (1961), which permits the validation of such a theory for both static and dynamic friction. Finally, as for Derevjanik (2001) it can be said that the function which connects friction coefficient with velocity has a different trend when the temperature varies. Another important phenomenon studied in previous years which is also temperature dependant, is that of stick-slip, to which clutches are subject and which creates unstable vehicle behaviour (see Ingram et al. (2011)). Therefore, it is very important to study thermal behaviour and, specifically, unsteady behaviour as compression between discs will not be continuous in time. Many researchers have followed a finite element analysis (FEA) approach to analyse the thermal behaviour for cases similar to that of a differential. A finite element thermal analysis of a ceramic clutch has been done by Czél et al. (2009) in which two independent finite element models are considered. These are linked by heat partition which changes in time and space. In this paper the authors consider heat generation as a distributed heat source and importance is given to changes in time and space of the heat convection coefficient. Another clutch, this time a multi-disc clutch, is analysed with a FE approach by Abdullah et al. (2015) and, specifically, its transient thermo-elastic behaviour, not only in the clutch discs but also in the pressure plate, plate separators and piston. The intent of this paper is to study the failure of the contact surfaces. The model used is a simplified but still very effective (since it is similar to real conditions) axisymmetric model. Considering similar transmission systems such as hydro-viscous drives, transient thermal analysis using a three-dimensional method has been approached by Cui et al. (2014). In this case, the heat flux generated between two adjacent friction pairs is considered to vary and is calculated from equilibrium considerations which allow calculation of the normal pressure between the surfaces. Great focus has been put on the heat conduction process. In this paper considerations on how the temperature profile varies axially and radially are done. A very interesting approach to solving the thermal transient problem with a finite element analysis is offered by Feng et al. (2013) where a face-based smoothed finite element method (FS-FEM) is used. With this method, it is possible to analyse the transient thermal problem using a three-dimensional approach with non-linear solids. The FS-FEM method is used since FE models are known to be overly-stiff as the model is discretized. Other numerical methods can be found in the literature to study the thermal behaviour of wet clutches. For instance, Jen and Nemecek (2008) use a separation of variables technique, which is then compared with an experimental model where thermocouples are used to measure the temperature in a power-shift transmission during one clutch engagement. The values measured have then been used to validate the numerical model. As already mentioned, there are many factors that influence the thermal behaviour of a clutch due to the different engagement conditions which occur. Therefore, it is important to take into consideration some characteristics of the components such as the waviness and roughness of the surface, and the deformability and permeability of the material (Jang and Khonsari (1999); Li et al. (2014)). Here it is shown how temperature rises considerably in a one second time scale. However, none of the papers described analyse the disc pack of a clutch in a semi-active differential and, most importantly, none of these characterize the temperature distribution of the discs' surfaces in unsteady conditions for various thermal loads. Since the temperature of the clutch itself is highly variable from disc to disc, the goal of this paper to study the distribution of temperature internal to the clutch considering each disc and, specifically, the temperature of the surfaces which take part in the generation of friction torque and consequently heat. This has been done considering the unsteady behaviour and characterizing the temperature distribution of the friction surfaces after a certain amount of time correspondent to the worst case scenario in terms of actuation time of the differential. Finally, to evaluate the need of an external cooling system, the disc pack's temperature has also been characterized as a whole with the evaluation of the average temperature reached during a duty cycle. Also, all the other heat sources in the differential which contribute to raising the temperature such as bearings, seals, gears and tripod joints are considered. The approach used in this research is a FE approach, where various conditions are analysed after having created a parametric axisymmetric model. Specifically, this has been done by using ANSYS Mechanical APDL.

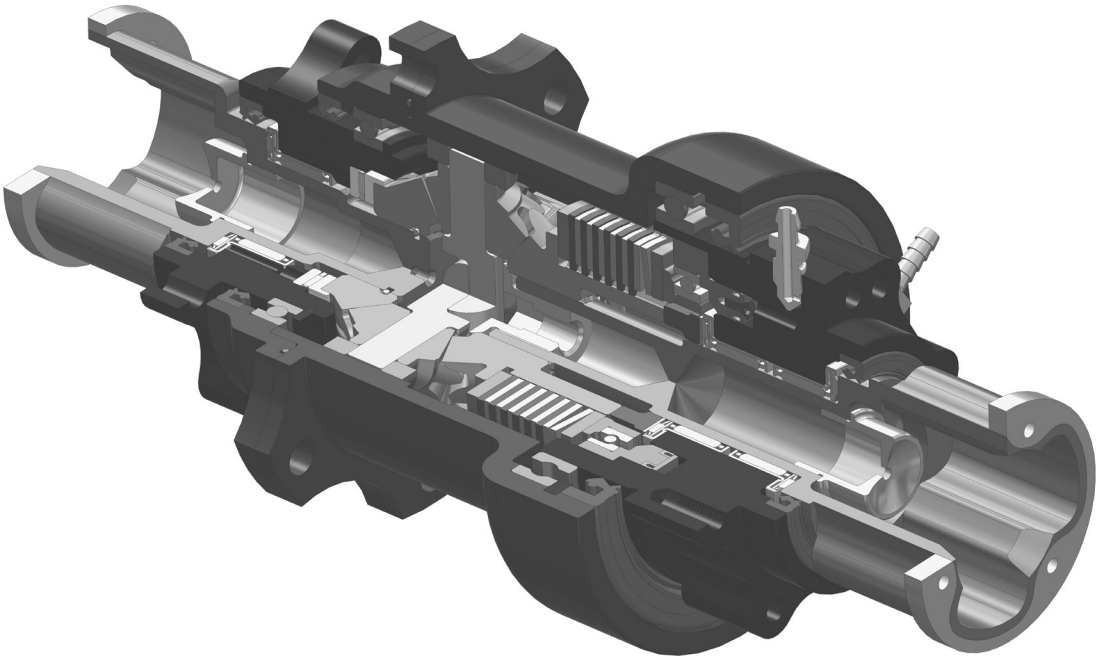

Fig. 1. Cutaway view of a SAD

Nomenclature

a_x	maximum longitudinal acceleration
A_a	apparent contact area
A	contact area
c_p	specific heat
d	internal diameter
D	external diameter
E	Young's modulus
f	friction coefficient
F	force
F_x	longitudinal force
F_{z_r}	vertical force on rear axle
h	vehicle center of mass height
H	heat transfer coefficient
HB	Brinnell hardness
h_c	contact conductance
H_c	contact microhardness
i_{rw}	number of ball crowns
l	characteristic length
m	vehicle mass

M	torque
M_d	maximum torque at differential
M_f	frction torque generated by the disc pack
M_m	gears transmitted torque
m_{sr}	vehicle static mass on rear axle
M_w	torque per wheel
p	pressure
$\dot{Q}$	heat transferred
r	wheel radius
R	curve radius
R_m	mean radius
s	effective surface slope
T	temperature
t_r	rear track
T_s	wall temperature
T_∞	bulk temperature
v	travel velocity
V	vehicle longitudinal speed
V_M	variable dependant on oil level
W	heat generated by friction
w_b	wheelbase
$z_p^\star$	planet equivalent circular gear number of teeth
$z_s^\star$	solar equivalent circular gear number of teeth
α	thermal diffusivity
η	efficiency
λ	thermal conductivity
μ_x	maximum longitudinal adherence coefficient
ν	Poisson's modulus
ρ	density
σ	effective surface roughness
$\Delta\tau$	time lapse
ω	rotational velocity
$\Delta\omega$	relative rotational velocity
ECU	Electronic Control Unit
FEA	Finite Element Analysis
FEM	Finite Element Method
FE	Finite Element
FS-FEM	Face-based Smoothed Finite Element Method
LSD	Limited Slip Differential
LVFA	Low Velocity Friction Apparatus
TCC	Thermal Contact Conductance
SAD	Semi-Active Differential

1.1. SAD working principle

The SAD assembly under study can be divided into three parts: a left and a right cartridge with a central housing. The left cartridge derives from a standard open differential and is composed of a solar gear, driveshaft, bushings and a carter which connects the cartridge to the chassis. The central housing is composed of a casing, cross and planet gears. The casing is rigidly connected to the final gear of the transmission, therefore, it receives torque directly from the engine. This torque is transmitted to the cross and planets, as these are obliged to rotate with the differential

Table 1. Vehicle parameters

Parameter	Description	Value	Unit
r	Wheel radius	254	mm
h	Vehicle centre of mass height	280	mm
m	Vehicle weight	300	kg
m_{sr}	Static mass on rear axle	180	kg
a_x	Maximum longitudinal acceleration	1.1	g
w_b	Vehicle's wheelbase	1600	mm

casing. As in all open differentials, the planets then engage with the solar gears transmitting torque to the half-shafts. The cross is not axially constrained, therefore, it is free to translate in the axial direction. Its position depends on the equilibrium of the reaction forces produced by the bevel gears. The right cartridge is composed of the clutch, a solar gear, half-shaft, bushings and a carter. The carter hosts the hydraulic piston, which represents the actuation system of the SAD. The piston chamber is part of the carter and is fed directly by the external hydraulic actuator. The piston is made of two parts, one is in contact with the friction discs and is free to rotate while the other is hosted in the chamber and can only translate. An angular contact bearing connects these two parts. The clutch is composed of twelve friction discs. Each disc is free to move axially according to the force produced by the actuator. However, the discs' rotation is constrained alternatively by the right solar gear and casing. Six discs rotate with the housing and six discs rotate with the right half-shaft. There are, therefore, eleven friction surfaces in the clutch. The clutch discs connected to the solar gear are treated with a molybdenum coating. This way, deterioration of clutch performance due to wear is minimized.

The actuator is an electrical actuator powered by an electric brushless motor that drives a ball screw actuating on a hydraulic piston. The oil compressed by this piston is directly connected with a hose to the hydraulic piston inside the differential. The vehicle parameters for which the differential analysed in this paper was developed can be seen in table 1.

2. Thermal analysis

2.1. Heat transfer

It is important to analyse the main thermal phenomena which occur during clutch engagement of the differential. Specifically, looking at the differential's construction in figure 1, it can be said that there are primary heat sources, represented by the clutch discs and secondary heat sources, represented by the bearings, gears, seals and tripod joints. The heat generated by the various sources will heat up all the components by transferring energy by conduction and convection. Finally, the heat will be dissipated to the external air in contact with the external casing and tripod joints of the differential. The equation governing the conduction heat transfer in space and time is the differential equation, known as Fourier equation (see Bergman and Incropera (2011)) in which thermal diffusivity α plays a primary role and can be defined as:

$$\alpha = \frac{\lambda}{\rho c_p} \tag{1}$$

In this paper, these equations were solved using a FEM approach and, specifically, by means of ANSYS Mechanical APDL. To solve these differential equations, it is necessary to impose the various boundary conditions in the FE model. Moreover, these are given by the heat transfer coefficient to characterize the convection heat transfer, thermal contact conductance and the various heat sources.

2.2. Convection

Concerning convection, a very simple formulation can be written as follows:

$$\dot{Q}_{conv} = HA\,(T_s - T_\infty) \tag{2}$$

The heat transfer coefficient is normally evaluated with similitude theory and using dimensionless parameters such as Reynolds number, Nusselt number, Prandtl number etc. Both the heat transfer coefficient for the lubricating oil and external air were applied in FE the model and evaluated as:

$$H_{oil} = 1000\frac{W}{m^2K}$$
$$H_{air} = 150\frac{W}{m^2K}$$

These values are consistent with what can be found in the literature (see Czél et al. (2009); Cui et al. (2014); Feng et al. (2013); Jang and Khonsari (1999)). Concerning bulk temperatures, the oil temperature is calculated by the FE model since it exchanges heat with the system and its temperature changes at each step of integration whilst the air temperature was considered to be constant and in standard conditions, i.e.

$$T_{air} = 25°C$$

2.3. Thermal contact conductance

Other boundary conditions to impose to the system are the thermal contact conductance. To represent the real amount of energy transferred due to conduction it is necessary to consider that the contact surfaces aren't ideal, i.e. same temperature of two separate bodies along the contact surface. In fact, a temperature drop can be observed in reality. This is due to the fact that the surfaces actually only touch along material asperities, so the heat exchanged depends on the relative roughness of the two surfaces in contact. This phenomenon is influenced by many factors, which can be intrinsic to the material or can be dependent on the working condition. The area of the contact patch clearly depends on the roughness and waviness of the two surfaces. Also, as the two adjacent elements are often pressed against each other, as in the case of a clutch or the SAD, the contact area will be subject to variations. These depend obviously on the pressure applied, but also on the local deformation state, so if the local contact areas are in elastic or plastic deformation states. This will change the equations that govern how the contact area changes. Finally, it can be said that other material properties which influence this phenomenon are hardness of the material (so also heat and chemical treatments of the object's surface), Young's modulus and Poisson's modulus. Also, external factors such as load cycling conditions or temperature will have an important influence. All of these considerations have been thoroughly studied to find the dependence of TCC on the various factors and to find correlations which give a mathematical formulation to it (see Wang and Zhao (2010); Sunil Kumar and Ramamurthi (2004); Yovanovich and Rohsenow (1967); Misra and Nagaraju (2010); Bahrami et al. (2005); Gopal et al. (2013); Tang et al. (2015);

Yovanovich (1981)). The most important and significant correlations, which are used in this work, are found by Sridhar and Yovanovich (1996).

$$TCC \equiv \frac{\sigma}{s}\frac{h_c}{\lambda_s} = 1.25\left(\frac{P}{H_c}\right)^{0.95} \tag{3}$$

With the effective surface roughness, effective surface slope and effective interface thermal conductivity being respectively:

$$\sigma = \sqrt{\sigma_1^2 + \sigma_2^2} \tag{4}$$

$$s = \sqrt{s_1^2 + s_2^2} \tag{5}$$

$$\lambda_s = \frac{2\lambda_1\lambda_2}{\lambda_1 + \lambda_2} \tag{6}$$

The subscripts 1 and 2 denote the surfaces or metals on either side of the interface. The relative contact pressure consists of the nominal pressure:

$$P = \frac{F}{A_a} \tag{7}$$

Therefore, depending on contact pressure, roughness, hardness and material properties, the various TCC for each contact and each condition of load (actuation pressure) were calculated and implemented in the FE model as a property of the elements which model the contacts.

2.4. Heat sources

Finally, the heat sources need to be estimated and assigned to the model. As in all transmission devices, there are many losses due to dissipative forms of energy in the differential which cause heat generation. This heat is not at all negligible if a proper analysis is to be done. Basically, in every contact where there is relative motion, heat will be generated, as there will always be some form of dissipative energy.

This regards components such as bearings, seals, gears and tripod joints. A cross section of the SAD is shown in figure 2 where all the heat sources are highlighted, apart from the tripod joints which will be considered in this work. Since the heat generated by the various heat sources depends on the force acting on the various components, many cases are evaluated. The two parameters which are considered as variable inputs are the pressure p of the actuation circuit and the relative rotational speed between the discs $\Delta\omega$. All of the other parameters such as longitudinal velocity of the vehicle or torque transmitted to the differential are considered as fixed parameters. It should be noted that working conditions change depending on which wheel is the slower wheel, as torque will be greater on one wheel or on the other. Consequently, one half of the differential (the one on the side of the slower wheel) will be subjected to higher loads. Also, since the discs of the clutch, and specifically the study of their temperature, are the main goal of this research, the worst working conditions for the discs are considered. Therefore, only conditions where the wheel on the side of the clutch, the right side, is the slower wheel are evaluated because in these conditions the right solar will receive a greater amount of torque and generate a greater axial force. This force will then act on the various heat sources on the right side of the differential, for instance, the bearings on the side of the actuation. By being subjected

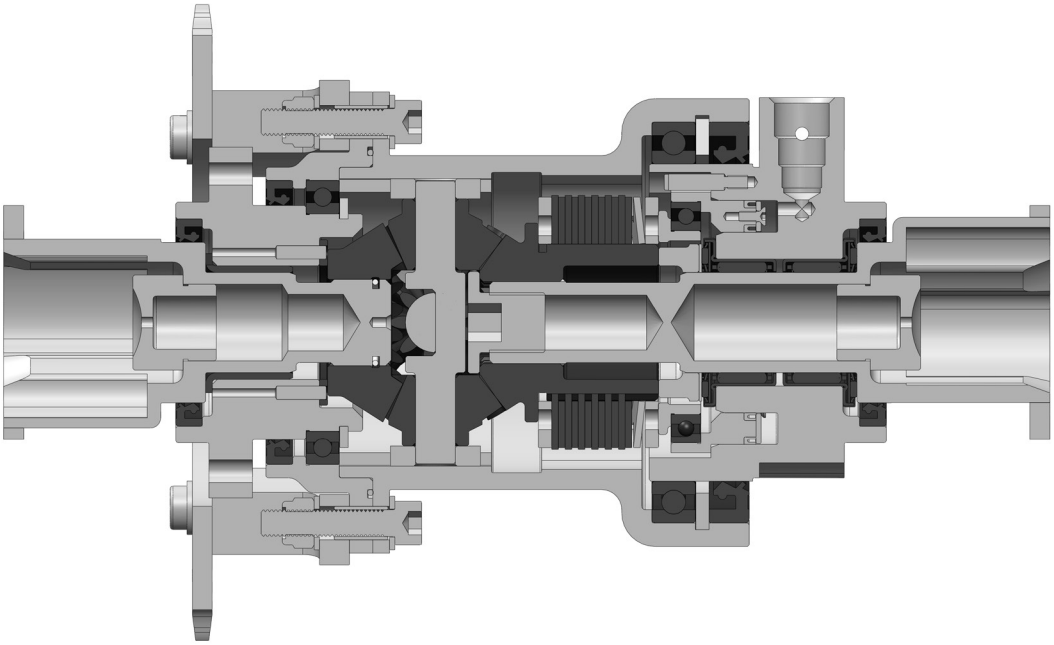

Fig. 2. Section of the SAD; the heat sources are highlighted as dark items

to higher stress, these bearings will consequently generate more heat. It must also be said that the TCC will be higher due to a higher pressure acting on the various contacts which increases the contact area and thus allows greater heat exchange for conduction through the components of the differential. This means that it is easier for heat to reach the components in contact with the external air and thereby making it less burdensome for the right side by lowering the temperature gradient. However, this effect is at least an order of magnitude lower than having a higher load on the heat sources and, consequently, a larger amount of heat produced. For these reasons, the case which is considered for all calculations is the one with higher loads on the right side of the differential (where the actuation and disc pack are places), so with the right wheel spinning at a slower rate. The chosen independent variables are pressure and relative rotational velocity between discs. Concerning pressure, the maximum actuation pressure is 20bar, so all the values of pressure from 1bar to 20bar are considered, with a discretization step of 1bar. Concerning the relative rotational velocity between discs $\Delta\omega$, considering kinematic conditions the following equation has been found:

$$\Delta\omega = \frac{Vt_r}{Rr} \tag{8}$$

where R is the curve radius (calculated as average of a skid pad). The conditions used to estimate the various thermal loads can be seen in table 2.

2.4.1. Primary heat sources

The main source of heat present in the differential is the disc pack. The amount of thermal energy produced by the discs is dependent on both the input variables: pressure and relative rotational velocity between discs. The relationship between the friction and heat generated by the clutch and the pressure in the piston chamber is quite clear. The same

Table 2. Forces applied

Parameter	Description	Value	Unit
F_{z_r}	Vertical force on rear axle	254	N
μ_x	Maximum adherence longitudinal coefficient	280	
F_x	Longitudinal force	300	N
M_w	Torque per wheel	180	N m
M_d	Maximum torque at differential	1.1	N m

thing can be said for the relative rotational velocity between adjacent discs. A simple but very effective way to consider the amount of friction and, therefore, heat generated by the discs is by considering Reye's hypothesis for which the heat generated due to friction can be found as follows:

$$W = M_f \Delta\omega = fFR_m \Delta\omega \tag{9}$$

2.4.2. Secondary heat sources

There are many other heat sources other than the clutch in the differential, specifically the bearings, gears, seals and tripod joints. The heat generated by the bearings can be calculated with simple equations given by bearing manufacturers. The bearings present in the differential are of many kinds: deep groove ball bearings, angular contact ball bearings, combined radial-axial needle roller bearings and journal bearings. Depending on the structural purpose of each bearing, the thermal load generated might depend or not on the actuation pressure. However, the relative rotational velocity doesn't influence the heat generated by any of the bearings. Generally, the heat generated is a function of many parameters:

$$W = W\left(F, \omega, v, d, D, i_{rw}, V_M\right) \tag{10}$$

The heat generated by the gears is dependent on both the independent variables considered and can be evaluated considering the efficiency of bevel gear engagement as follows:

$$\eta = -f\pi\left(\frac{1}{z_p^\star} + \frac{1}{z_s^\star}\right) \tag{11}$$

where $z_s^\star$ and $z_p^\star$ are respectively the number of teeth of the solar and planet gears when considering an equivalent circular gear which is done by considering Tredgold's method. It is then possible to evaluate the heat generated by the gears as:

$$W = \Delta\omega_{s-p}\left(1 - \eta\right) M_m \tag{12}$$

Where $\Delta\omega_{s-p}$ is the relative rotational velocity between the planet and solar gears. The heat generated by the seals is instead independent of both the independent variables of the problem and can be evaluated using manufacturers appropriate tables. It depends only on rotational velocity of the shaft ω and shaft's diameter d:

$$W = W(d, \omega) \tag{13}$$

Finally, the heat generated by the tripod joints depends the transmitted torque and, therefore, the actuation pressure. To quantify it, it is considered that in a complete rotation of the wheel, the suspension executes a complete extension and compression cycle, meaning that the joint executes its maximum travel twice. Therefore, it can be written as a function of transmitted torque and travel velocity as follows:

$$W = W(M, \omega) \tag{14}$$

3. FE model

The FE model of the differential which is developed is an axisymmetric model. This simplification can be justified considering that most of the components are cylindrical components and therefore symmetric relative to their axis. The fact that the FE model is axisymmetric and thermal (only one degree of freedom per node) allows to have a model with low computational cost. This fact is very important since unsteady (necessary to analyse the differential) analysis of such complex geometries are very heavy in terms of computational cost. Nevertheless, the simplified model, preserves the characteristics of the model, allowing to analyse many cases in terms of load. Some components, however, are not cylindrical or symmetric relative to their axis, so for these components some simplifications are considered, for instance, as concerns the materials properties, as the geometry is not the actual one. To consider the differences between the real model and the FE axisymmetric model some modifications to the real material properties have to be applied to those components which are not axisymmetric. Concerning density, which influences only the unsteady behaviour, an equivalent density is calculated with a simple proportion based on the fact that the mass of the real component and the one in the axisymmetric model have to be equal, so the equivalent density is found with a simple proportion between volumes. Concerning conductivity and specific heat capacity, which influence both steady and unsteady conditions, a weighted average is calculated. This is done considering that the axisymmetric component is a complete revolution of a two-dimensional area whereas the real component is composed of angular sectors of oil and angular sectors of the component materials. The weights of the weighted average used are thermal conductivity or specific heat capacity of the various materials, respectively λ_i and c_{p_i}.

$$\begin{cases} c_{p_{eq}} = \dfrac{\sum_{i=1}^{n} c_{p_i} l_i}{\sum_{i=1}^{n} c_{p_i}} \\ \lambda_{p_{eq}} = \dfrac{\sum_{i=1}^{n} \lambda_{p_i} l_i}{\sum_{i=1}^{n} \lambda_{p_i}} \end{cases} \tag{15}$$

The complete geometry and mesh of the axisymmetric model can be seen in figure 3. Great importance is given to the mesh of the discs, where strong temperature gradients are present.

To this FE model, the various boundary conditions previously discussed were applied. The element type used to model the various components is PLANE55, whereas the contacts were modelled using CONTA171 and TARGE169 elements. The lubrication oil and actuation oil are modelled as two single masses containing the respective fluids characteristics in terms of thermal properties. These masses are then connected to the elements with which they

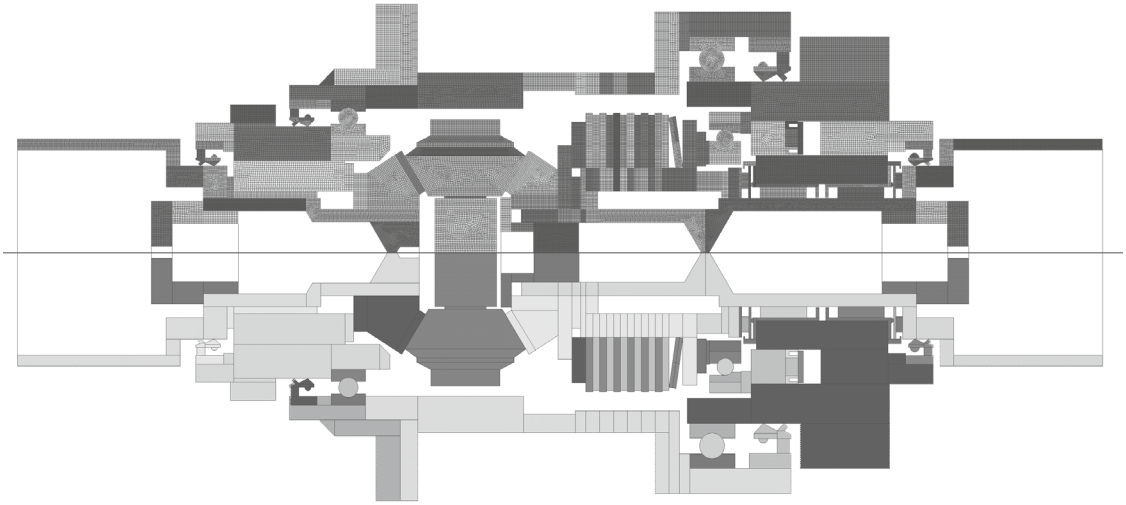

Fig. 3. Mesh of the complete geometry

Table 3. Material properties

Material	$\rho\left(\frac{kg}{m^3}\right)$	$c_p\left(\frac{J}{kgK}\right)$	$\lambda\left(\frac{W}{mK}\right)$	HB	$E\,(GPa)$	ν
C45	7870	500	54	440	210	0.27
C45 with molibdenum coating	7870	500	54	740	210	0.27
Ergal (7075-T6)	2810	915	155	160	72	0.33
36NiCrMo16	7840	460	33	518	208	0.27
18NiCrMo5	7850	460	41	582	210	0.27
Rubber	1500	1.6	0.2			
Oil $(25°C)$	858	2000	0.15			
Air $(25°C)$	1.165	1005	0.026			

exchange energy. This approach allows to consider the variation of temperature (bulk temperature for convection heat exchange) of the two oils due to the various heat exchange processes. The modelling of the two lubricators is very important because of its thermal inertia. Moreover, the oil present in the differential will tend to uniform the temperature inside the differential, especially once the unsteady behaviour tends to stabilize. In fact, considering small time lapses, the oil will have little effect considering its very low thermal diffusivity, vice versa, it will have a higher effect when almost steady state conditions are reached or when the temperature stabilizes during a duty cycle. The mass element used is a MASS71 element which is the connected with LINK34 element types to the various component with which the oil exchanges heat. The total number of elements present in the model is 57061 whereas the number of nodes is 54432 The material properties considered in this work can be seen in table 3.

A very important role is played by the contacts which are characterized by thermal contact conductance TCC. This is an input value which must be supplied to the model when defining the various contacts between the components. There are many models to evaluate TCC. In this work, Yovanovich's correlations are used. The parameters which need to be known to calculate TCC with these correlations are:

- pressure at contact
- Brinell hardness for the two components
- Young's modulus for the two components
- Poisson's modulus for the two components
- roughness of the two contacting surfaces

Most of the parameters for Yovanovich's correlations depend on material properties, and surface and heat treatments, and are, therefore, fixed parameters. The same thing cannot be said for the pressure between the contacting components that mostly depends on the pressure of the actuation oil, so the instantaneous locking percentage. The value of TCC varies due to the many different pressure conditions evaluated as each contact depends on pressure in a different way. For instance, there is a direct dependency on pressure between two discs, whereas between the discs and casing, this value depends on the torque transmitted which depends on the friction torque and so ultimately on the actuation oil pressure. The situation is the same for bearings, gears and all the other components. All of these factors were taking into consideration when applying the boundary conditions to the model.

4. Reasults and discussion

4.1. Steady state

The first analysis done is the case of steady-state. When steady-state conditions are reached, the amount of heat entering the object exactly equals the one exiting; therefore, no energy is used to raise the object's temperature. These conditions are an asymptotic value, meaning that they are reached only in a very large time scale. However, for this kind of differential, these conditions never occur since the loading conditions change continuously. A steady state analysis is important because it shows for each of the various conditions what the hottest parts in the whole differential are and how the radial and axial distribution of temperature on the disc surfaces stabilize over time. The first case analysed is where no heat flux is generated by the clutch, so as if it were an open differential run for many hours. From this analysis, it can be seen how heat fluxes deriving from bearings, seals and gears influence the thermal behaviour of differentials. Seal temperatures tend to be very high, because standard rubber is considered due to the absence of data on seal material while, in reality, these are designed for sliding contacts and are, therefore, very resistant to heat. This kind of analysis is important since the clutch internal to the differential cannot be actuated for many hours, for instance during a drive along a motorway. Therefore, a steady-state analysis is fundamental to study how heat is dissipated in such conditions, without the contribution of the heat generated by the disc pack. It can be seen that fluxes due to bearings and seals are important as they raise the initial temperature of the system by $15°C$ to an initial temperature of approximately $40°C$. A slightly higher temperature can be seen in the area where gear contact occurs. The temperature of the casing was measured during experimental testing of the differential without actuation, and was found to be approximately $40°C$, which validates this model. In figure 4, the steady-state analysis is shown.

At this point, the steady-state analysis results of conditions with pressure in the piston chamber, so when working as a locking differential, can be analysed. The analysis is run for pressure values p of $1; 4; 8; 12; 16; 20$bar and for each pressure value, the relative rotational velocities of the discs $\Delta\omega$ of $0.5; 1; 1.5; 2; 2.5; 3\frac{rad}{s}$ are considered. Therefore, a total of 36 load cases are considered. It should be noted that any time one of these values changes, not only do the heat fluxes affected by these parameters change, but also other values of the model such as TCC. The same considerations are made for the case in which the relative velocity between the discs is kept fixed and the variable parameter is the pressure in the piston chamber.

4.2. Unsteady-state analysis

The most important results of this research are obtained considering unsteady-state conditions. Therefore, the results obtained from the simulation can now be focused on. Many different kinds of simulations are run to properly study the phenomenon. The main goal is to obtain the temperature distribution of the friction surfaces of the disc pack in both the radial and axial direction after a certain amount of time of a certain load being applied. The amount of time for which the load is applied and after which the disc pack temperature distribution is analysed considered in this paper is the most critical in terms of differential actuation in terms of continuous actuation time. This time lapse has been measured from experimental tests (telemetry data) and corresponds to $10s$. Therefore, the results shown are instantaneous conditions of the differential after $10s$ of continuous loading starting from standard conditions. With these results the local temperature for each contact surface can be known, so the effective friction torque generated can also be found with other appropriate models (which include other phenomena other than heat). The reason why instantaneous conditions have been evaluated rather than the trend in time of the temperatures, is that the SAD works

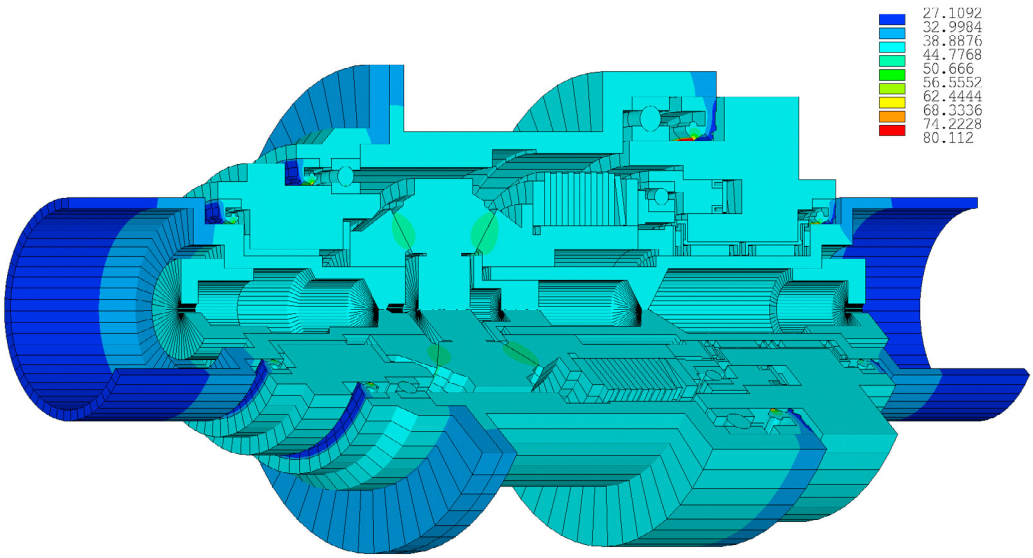

Fig. 4. Steady-state analysis of the differential without actuation

in many different conditions, so it would be impossible to characterize every conditions. What instead is of interest is the temperature distribution of the friction surfaces after a characteristic actuation time and what is that average temperature of the disc pack during a duty cycle to evaluate the need of an external cooling system. Considering the temperature distribution of the friction surfaces after 10s, the temperature for all the 36 conditions of pressure and relative rotational velocity between the discs are analysed. It is interesting to view which temperature values are reached but also how the temperature gradient behaves. This allows the result to be independent of the time lapse considered. Only one condition will be described and analysed in-depth, specifically the worst conditions of heat flux. All the other conditions, which have been analysed, will give the same results but with different number, therefore, the results will be omitted. The case considered for the moment is:

$$\begin{cases} p = 20 \text{ bar} \\ \Delta\omega = 3.0 \dfrac{\text{rad}}{\text{s}} \end{cases} \tag{16}$$

The first interesting thing to investigate is how the temperature varies along the radius for each disc. In figure 5 the temperature distribution for the contact surfaces of the discs are shown. Concerning the axial direction, the origin has been considered to be the closest contact surface to the preload Belleville spring sited on the far right of the pack. It can be noticed that the temperatures decrease going towards the solar gear.

After having seen how the temperature varies along the radius for the various friction surfaces, it can be said that, as expected, the hottest part is at the centre of the discs, in both the radial and axial direction. This is justified by the fact that in the centre of the disc pack, the heat generated by the discs can only exit radially since in the axial direction it receives additional heat from the adjacent discs instead of them dissipating it. All the physical phenomena included in the heating process validate this model. In fact, because of the different values of thermal diffusivities in such a small amount of time as the one considered, it is clear that heat tends to exit the differential through the casing which is made of aluminium and is in direct contact with the external air. However, also for small radii, the temperature is lower because in this area there is direct contact with a large mass such as the solar gear, so a lot of heat is absorbed

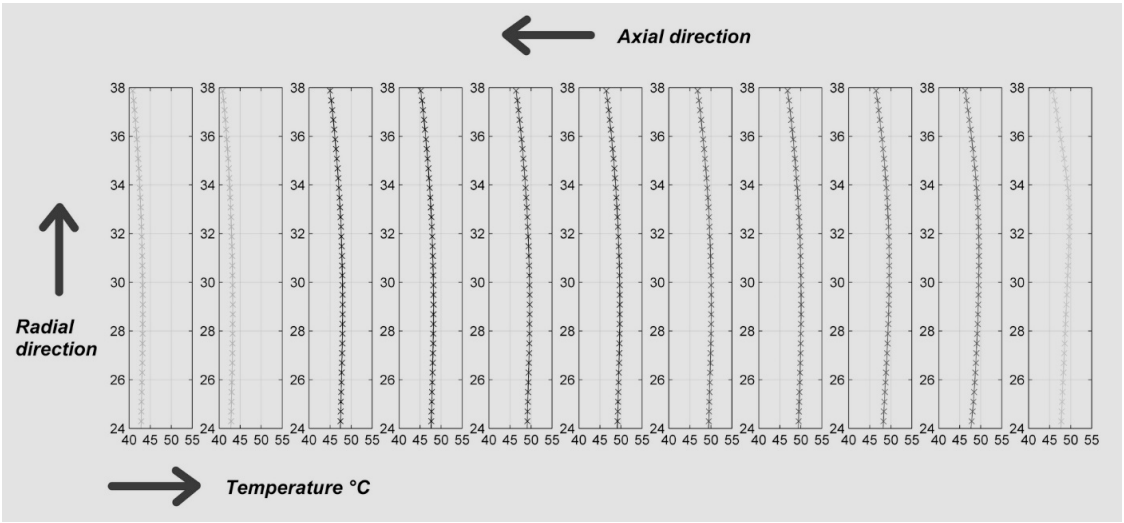

Fig. 5. Disc surfaces radial temperature distribution

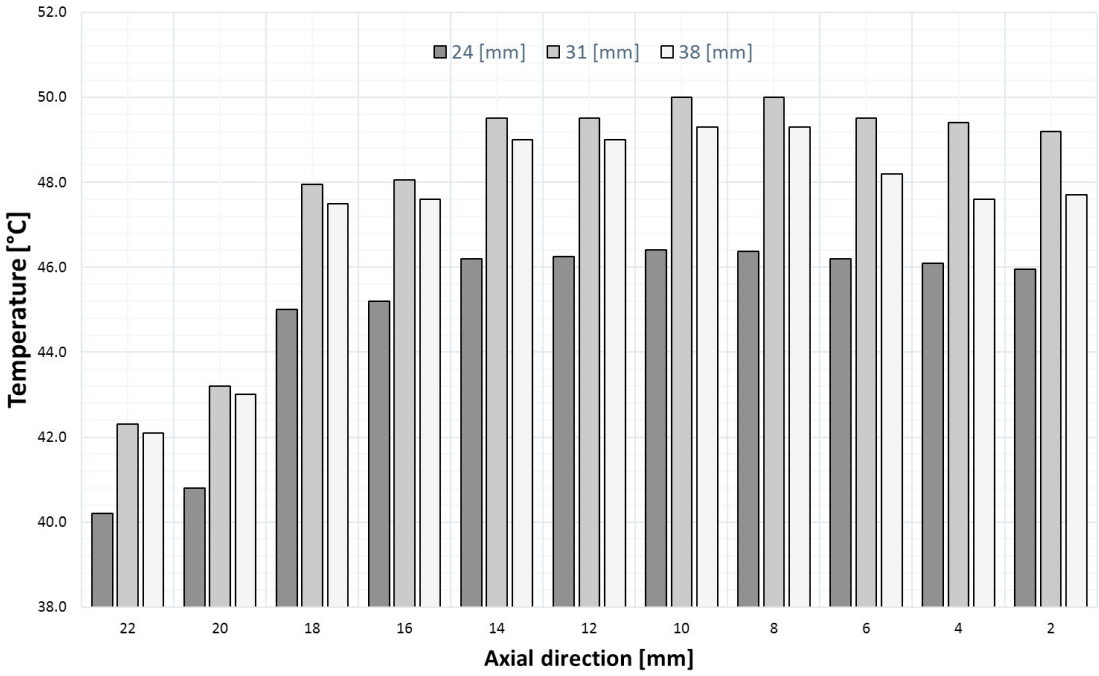

Fig. 6. Internal disc axial temperature distribution for various radii

by this component. This is the same reason for the fact that the discs closer to the centre of the differential are cooler. Another interesting plot can be created considering the axial temperature distribution for a fixed radius. this is shown in figure 6.

Once again the results obtained are justified by the physics laws governing this phenomenon. The legends indicate various radii for which the results have been plotted. All statements previously made are demonstrated in these plots. The temperature is higher towards the middle of the disc pack and decreases particularly going towards the solar gear. As regards increasing radii, temperature increases until a certain radius after which it decreases again. At this

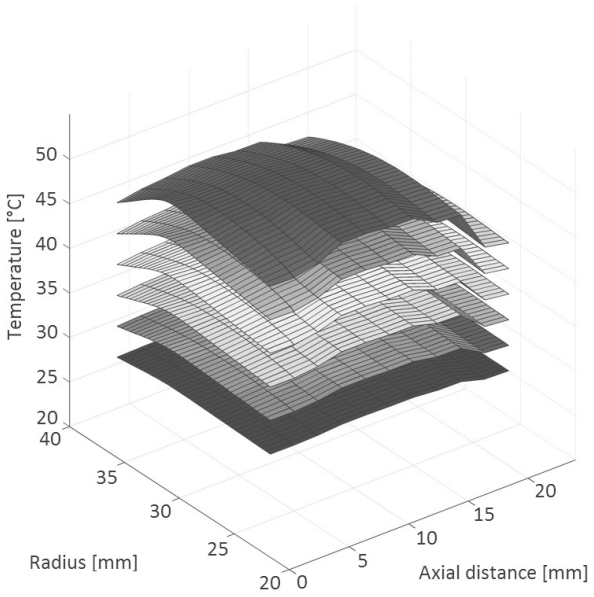

Fig. 7. Temperature maps of the disc pack for a pressure of 20bar

point, three-dimensional maps can be created by putting the bi-dimensional plots together. These maps summarize the behaviour of the discs under various conditions of pressure and relative rotational velocity between the discs. Maps for a certain pressure for various $\Delta\omega$ have been overlapped which makes it is possible to compare the effects of the relative rotational velocity. In fact, large differences are noticeable when varying the relative rotational velocity. These maps characterize the clutch of the differential after 10 s of actuation. Therefore, using these maps it is possible to know what the local value of temperature is for each surface. At this point, by using adequate correlations, the real value of friction torque can be evaluated. Maps for the various cases considered are shown in figure 7; each plot represents a certain value of pressure, meanwhile each surface in the plot represents a certain value of $\Delta\omega$ (increasing from a lower value to a higher one as temperature grows). From these maps, it can be noticed that temperature is more pronounced towards the centre of the pack as it increases with both pressure and relative rotational velocity between the discs. Only the contact surfaces involved in the generation of friction torque have been considered.

As these maps are obviously time-dependant, to eliminate this dependency, a temperature gradient can be considered instead of absolute temperature. This is useful as it generalizes the problem and it can be used to establish the local friction coefficient and, therefore, calculate the effective friction torque generated considering also the influence of temperature. This kind of map is shown in figure 8.

To characterize the disc pack thermally, further considerations have to be done. A certain temperature distribution will be present along the radius as seen in previous plots. Consequently, depending on the axial position, each disc will tend to have a different temperature from the average temperature of the disc pack because of differing quantities of heat entering and exiting each disc. An average temperature for the disc pack can be found after a certain time lapse, again 10 s. This is the sum of the temperatures of all the FE model nodes representing the disc pack divided by the number of nodes. This temperature can be representative of the actual disc pack. However, each disc will tend to have a range of temperatures along the radius different to the average disc pack temperature by a certain quantity. Therefore, an approach to quantify this difference is studied. Specifically, for every thermal load condition considered and for every contact surface of the discs generating friction, the ratio between the difference in maximum and minimum temperature along the radius of a surface and the average temperature of the disc pack under the condition considered is evaluated. This way this ratio can be plotted for every condition to see how it varies in the axial direction and when

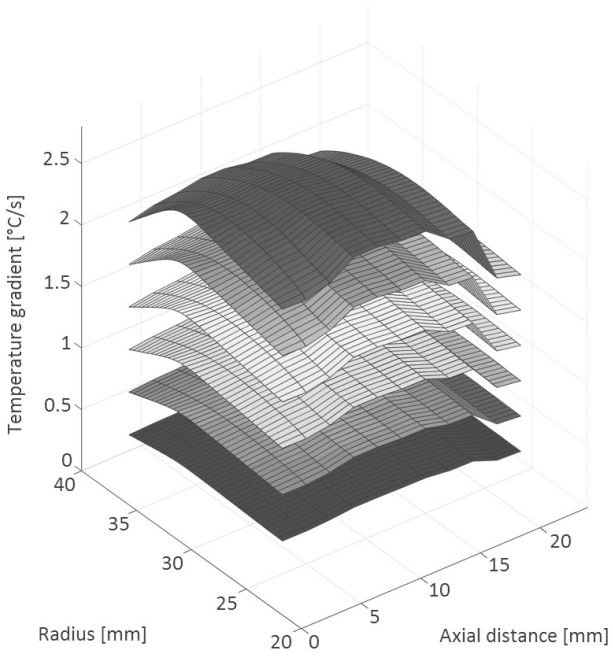

Fig. 8. Temperature gradient maps of the disc pack for a pressure of 20bar

varying pressure and relative velocity between the discs. This is done firstly on a plane, evaluating how this ratio varies with the variation in relative rotational velocity under a single pressure condition. For a pressure of 20 bar this is shown in figure 9.

The ratio considered is equal to:

$$\frac{T_{av_{disks}}}{T^i_{max}(r) - T^i_{min}(r)} \tag{17}$$

where $T_{av_{disks}}$ represents the average temperature of the disc pack and $T^i_{max}(r)$ and $T^i_{max}(r)$ the maximum and minimum temperatures for the i^{th} contact surface along the radius, respectively. The smaller this value is, the bigger the difference between the maximum and minimum surface temperature. Therefore, looking at the plots, it can be said that the larger the amount of heat produced by the clutch, the lower this ratio is. This is exactly the results shown in the temperature maps shown above, where temperature has a higher value towards the centre of the disc pack compared to the outside parts when the heat produced by the clutch increases. Also, in the axial direction of the disc pack, a local minimum of these curves can be found in the middle of the disc pack whereas the global minimum is on the surface in contact with the lubricant oil. Once again, three-dimensional maps can be created to summarize the result obtained for various conditions of pressure. Analysing different pressure loads, it can be noticed that increasing the pressure decreases the value of this ratio for all relative rotational velocities which also influence the ratio by decreasing it as they increase. The map in figure 10 shows the maps of this ratio for a fixed value of pressure.

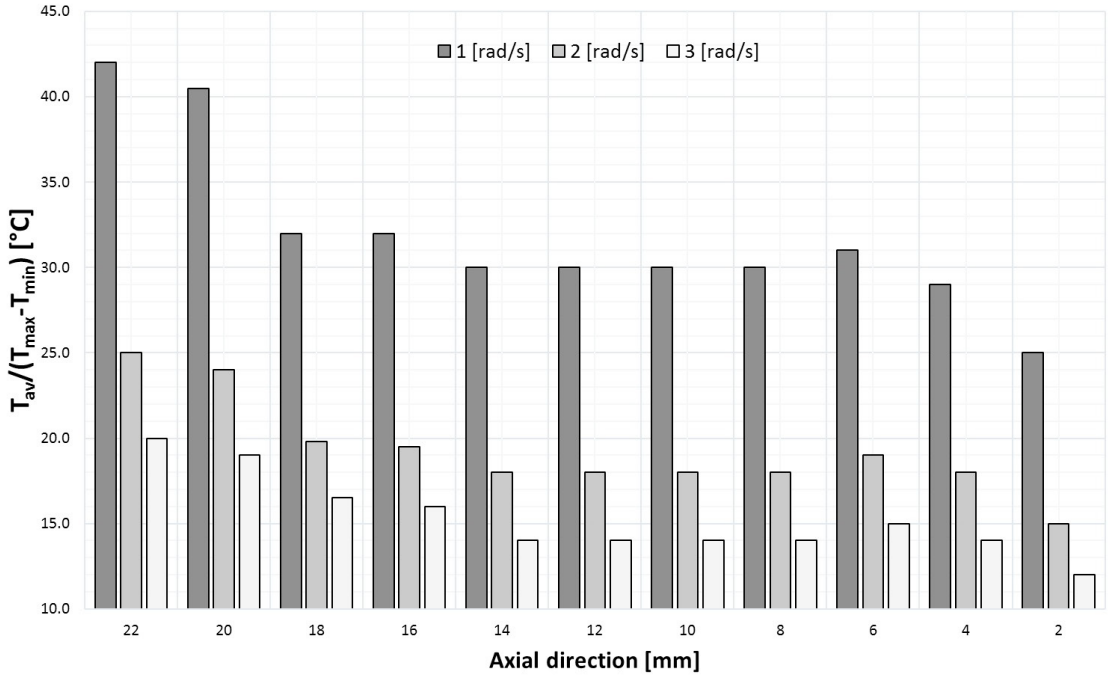

Fig. 9. Difference between average temperature of the disc pack and each disc for the external discs

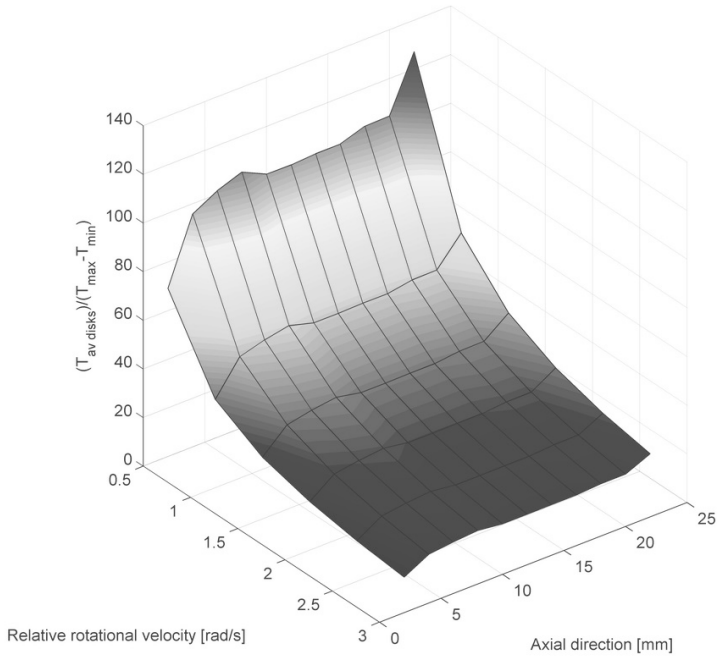

Fig. 10. Difference between average temperature of the disc pack and each disc for a pressure of 20bar

4.3. Duty cycle

The real working conditions of the differential change continuously. Although the analyses described so far do give interesting results for disc temperature and how it varies in the various directions, they do not give a value of the maximum temperatures that the disc pack will reach. This value, however, is very important since it allows to evaluate if an external cooling system is needed. It was decided to characterize and study disc pack thermal behaviour under cyclical working conditions by running a duty cycle with a realistic loading phase (actuation time of the piston) of 0.5 s and unloading phase (time where only the heat generated by bearings and gears is present) of 3 s. Also these time steps were evaluated experimentally. When studying a duty cycle, the transitory phase is expected to stabilize after a while. At the start, temperature increase during the loading phase will be higher than temperature decrease during the unloading phase. However, as the average temperature increases, its growth over time will decrease because the heat dissipated into the external air increases with the increase in average temperature. The same thing happens during unloading with an even more pronounced effect as there is no thermal load due to the clutch (which is the main source of heat production but does not contribute in this phase). Basically, the amount of heat exiting will increase due to the large temperature difference between the differential and external air, so during loading the temperature to time function tends to flatten out (since load application is constant, temperature rise decreases) while during unloading, the function tends to become steeper with time. At a certain point, these two quantities balance out as the temperature rise during loading exactly equals the temperature drop during unloading. In this case, the hottest node of the disc pack is used to characterize the thermal duty cycle of the differential. To make the simulation less data-intensive for computation, only one cycle is studied using the FE model, after which, the duty cycle curves are recreated by applying simple energy equilibrium equations. The equations considered for the loading phase are the following:

$$\begin{cases} Q_{in} - Q_{out} = \Delta\tau_1 mc_p \left(T_1 - T_0\right) \\ Q_{out} = -c_1 \left(T_0 - T_{air}\right) \end{cases} \tag{18}$$

Whereas for the unloading phase, the following equations have been considered:

$$\begin{cases} Q_{out} = \Delta\tau_2 mc_p \left(T_1 - T_2\right) \\ Q_{out} = -c_2 \left(T_1 - T_{air}\right) \end{cases} \tag{19}$$

where $\Delta\tau_1$ and $\Delta\tau_2$ are the time considered for the two phases, respectively loading and unloading. Q_{in} and Q_{out} are respectively heat entering (due to the clutch) and heat exiting the differential. T_0 is the temperature at loading cycle start, T_1 is the temperature at loading cycle finish equal to unloading cycle start and T_2 is the temperature at unloading cycle finish. These are evaluated with the FE model, after which, the constants k_1 and k_2 which characterize the heat transfer were found by solving the indicated systems. Once the constants are found, the whole duty cycle is created. Considering maximum heat fluxes for the loading phase, so 20 bar and $3\,\frac{\text{rad}}{\text{s}}$, a loading conditions plot can be created. Subsequently applying these loads, the expected result is obtained. To obtain realistic results, more than one cycle for the duty cycle is calculated from the FE model. This way, the values of constants c_1 and c_2 can be adjusted to calibrate the results to the numerical model. To obtain the real values of these constants without having to adjust them, very small time steps would have had to be considered. In the calculation described, the difference in temperature of the whole cycle is used to calculate Q_{out}; whereas to find the real amount of this heat, the time step would have had to be discretized in a much finer way. Alternatively, the constants can be adjusted by using more data, which is what has been done in this case. Therefore, the values are adjusted so that a ±0.5°C precision is guaranteed within the first five cycles which can be considered to be a precise result when studying thermal behaviour. In the thermal duty cycle shown in figure 11, the temperatures reached are quite close to those previously described where a fixed thermal load was applied, considering that a 1 : 6 loading to unloading time is used. In this plot, the average temperature during the cycle (in red) is also plotted. When the duty cycle stabilizes, a difference in temperature between the maximum and

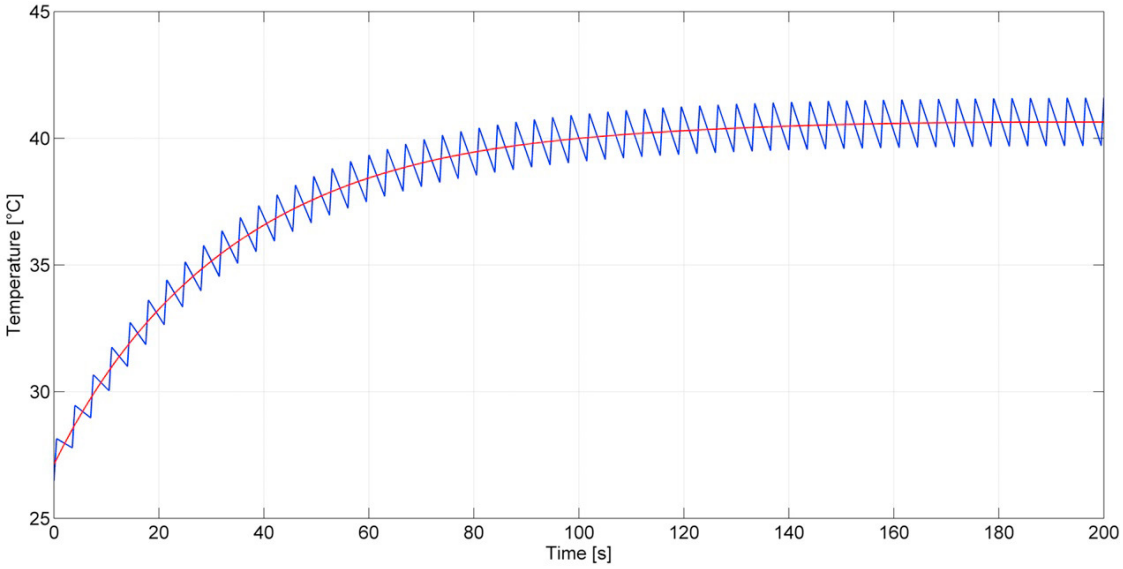

Fig. 11. Thermal duty cycle

the minimum of approximately 2°C can be seen. The average temperature reached by the disc pack is approximately 40°C. At this temperature the properties of the materials remain the same and, therefore, the correct functioning of the device is guaranteed. For this reason, an external cooling system is not needed.

5. Conclusions

Many different aspects regarding the thermal behaviour of a semi-active differential have been analysed in detail in this work. After having analysed the various heat sources and equations involved, the finite element model developed has been discussed. All the approximations, simplifications, hypothesis and techniques used to model the differential in the FE environment have been described. From the results, it can be said that the temperature gradient in the disc pack increases with the increase of heat produced by the clutch and the temperature tends to increase particularly towards the middle of the disc pack. Thermal maps of both the temperature distributions and the temperature gradients have been created for various working conditions. This has also been done to evaluate how the temperature along each surface differs in terms of surface temperature uniformity if compared to the average temperature of the entire clutch. This analysis, evaluated for a certain time lapse, is useful to evaluate the total friction coefficient and, consequently, the total friction torque generated by the disc pack considering the temperature influence. In addition, a duty cycle simulating real working conditions has been run to evaluate the temperatures reached by the entire pack, represented by the hottest node, after a certain amount of cycles so that the temperature increment during the loading phase is the same as the temperature drop during the unloading phase.

References

Abdullah, O.I., Abd Al-Sahb, W., Al-Shabibi, A., 2015. Finite Element Analysis of Transient Thermoelastic Behavior in Multi-Disc Clutches. doi:10.4271/2015-01-0676.

Bahrami, M., Yovanovich, M.M., Culham, J.R., 2005. Thermal contact resistance at low contact pressure: Effect of elastic deformation. International Journal of Heat and Mass Transfer 48, 3284–3293.

Bergman, T.L., Incropera, F.P. (Eds.), 2011. Fundamentals of Heat and Mass Transfer. 7th ed ed., Wiley, Hoboken, NJ.

Cui, J., Wang, C., Xie, F., Xuan, R., Shen, G., 2014. Numerical investigation on transient thermal behavior of multidisk friction pairs in hydro-viscous drive. Applied Thermal Engineering 67, 409–422.

Czél, B., Váradi, K., Albers, A., Mitariu, M., 2009. Fe thermal analysis of a ceramic clutch. Tribology International 42, 714–723.

Derevjanik, T.S., 2001. Detergent and Friction Modifier Effects on Metal/Metal and Clutch Material/Metal Frictional Performance. doi:10.4271/2001-01-1993.

Feng, S., Cui, X., Li, G., 2013. Transient thermal mechanical analyses using a face-based smoothed finite element method (FS-FEM). International Journal of Thermal Sciences 74, 95–103.

Gopal, V., Whiting, M., Chew, J., Mills, S., 2013. Thermal contact conductance and its dependence on load cycling. International Journal of Heat and Mass Transfer 66, 444–450.

Haviland, M., Rodgers, J., 1961. Friction characteristics of automatic transmission fluids as related to transmission operation. Lubrication Engineering 17, 110.

Hsu, S., Gates, R., 2005. Boundary lubricating films: Formation and lubrication mechanism. Tribology International 38, 305–312.

Ingram, M., Reddyhoff, T., Spikes, H.A., 2011. Thermal Behaviour of a Slipping Wet Clutch Contact. Tribology Letters 41, 23–32.

Jang, J.Y., Khonsari, M.M., 1999. Thermal Characteristics of a Wet Clutch. Journal of Tribology 121, 610.

Jen, T.C., Nemecek, D.J., 2008. Thermal analysis of a wet-disk clutch subjected to a constant energy engagement. International Journal of Heat and Mass Transfer 51, 1757–1769.

Li, M., Khonsari, M., McCarthy, D., Lundin, J., 2014. Parametric analysis for a paper-based wet clutch with groove consideration. Tribology International 80, 222–233.

Mäki, R., 2005. Wet Clutch Tribology - Friction Characteristics in Limited Slip Differentials. Ph.D. Thesis. Luleå University of Technology. Luleå.

Misra, P., Nagaraju, J., 2010. An Experimental Study to Show the Effect of Thermal Stress on Thermal Contact Conductance at Sub-megapascal Contact Pressures. Journal of Heat Transfer 132, 094501.

Ohtani, H., Hartley, R.J., Stinnett, D.W., 1994. Prediction of Anti-Shudder Properties of Automatic Transmission Fluids using a Modified SAE No. 2 Machine. doi:10.4271/940821.

Rudnick, L.R. (Ed.), 2017. Lubricant Additives: Chemistry and Applications. Chemical industries. third edition ed., CRC Press, Taylor & Francis Group, Boca Raton.

Sridhar, M., Yovanovich, M., 1996. Empirical methods to predict Vickers microhardness. Wear 193, 91–98.

Sunil Kumar, S., Ramamurthi, K., 2004. Thermal contact conductance of pressed contacts at low temperatures. Cryogenics 44, 727–734.

Tang, Q., He, J., Zhang, W., 2015. Influencing factors of thermal contact conductance between TC4/30CrMnSi interfaces. International Journal of Heat and Mass Transfer 86, 694–698.

Tesi, A., Vinattieri, F., Capitani, R., Annicchiarico, C., 2016. Development of an e-LSD Control Strategy Considering the Evolution of the Friction Torque with the Wear Depth. SAE International Journal of Engines 9.

Wang, A., Zhao, J., 2010. Review of prediction for thermal contact resistance. Science China Technological Sciences 53, 1798–1808.

Watts, R., Nibert, R., 1992. Prediction of Low Speed Clutch Shudder in Automatic Transmission Using the Low Velocity Friction Apparatus. MECHANICAL ENGINEERING-NEW YORK AND BASEL-MARCEL DEKKER- , 732–732.

Yovanovich, M., 1981. Thermal contact correlations, in: 16th Thermophysics Conference, American Institute of Aeronautics and Astronautics, Palo Alto, CA, U.S.A.

Yovanovich, M., Rohsenow, W., 1967. Influence of Surface Roughness and Waviness upon Thermal Contact Resistance. Technical Report 6361-48. Department of Mechanical Engineering, MIT.